SUPPLEMENTAL INFORMATION

Protease OMA1 Modulates Mitochondrial Bioenergetics and Ultrastructure through Dynamic Association with MICOS Complex

Martonio Ponte Viana, Roman M. Levytskyy, Ruchika Anand, Andreas S. Reichert and Oleh Khalimonchuk

Supplemental Figure Legends

Figure S1, related to Figure 1. BioID analysis of OMA1 physical interactome. (A) Top, Schematic depiction of OMA1-BirA construct used in BioID proximity labeling analysis. Bottom, List of relevant proteins identified by BioID proteomic analysis. **(B)** HEK293T cells were transfected with OMA1-GFP construct or mock transfected. Mitochondrial lysates from the respective cells were subjected to immunoprecipitation with anti-GFP magnetic beads. Precipitated proteins from the initial sample (load), unbound fraction (unbound), last wash (wash), and eluate were analyzed by western blot with indicated antibodies.

Figure S2, related to Figure 2. Stability of high-mass MICOS complexes is compromised in *oma1*$^{-/-}$ cells. (A) Schematic depiction of MICOS machinery and its partner protein complexes forming an IM-OM contact site. Some proteins are not shown for simplicity. **(B)** Mitochondrial lysates from WT and *oma1*$^{-/-}$ fibroblasts were analyzed by blue-native gel electrophoresis and immunoblotting with antibodies against indicated MICOS subunits as well as respiratory complex V subunit ATP5A (loading control).

Figure S3, related to Figure 3. MICOS-deficient cells exhibit altered cristae morphology characterized by concentric membrane stacks and lack of cristae junctions. Representative

TEM images of mitochondria in WT (left) and MIC13 knockout (right) HEK293T cells. Scale bars, 0.5 μm.

Figure S4, related to Figure 4. Quantitative assessment of cell survival by flow cytometry. (A) Viability over indicated periods of time of WT and *oma1*$^{-/-}$ fibroblasts with or without stable mitoT expression. Cells (500,000) were seeded per well in a 6-well plate. Growth was monitored for 3 days until over-confluence was reached. Events (10,000) were counted using Hoechst 33342 and propidium iodide staining parameters; healthy cells were PI-negative and Hoechst 33342-positive. Hoechst 33342-negative cells were not accounted for. Error bars, mean ± S.D. of n=3 biological replicates. **(B)** Steady-state levels of mitoT-GFP, OMA1, OPA1 and HSPD1 (loading control) in indicated cells that were incubated with or without 2 μM CCCP. Note that mitoT undergoes additional processing in the WT MEFs.

Figure S5, related to Figure 5. Bioenergetic deficit in *oma1*$^{-/-}$ cells is not directly related to **(A)** Steady-state levels immunoblot analysis of OMA1, YME1L, GAPDH and Myc-tagged OPA1 variant lacking S1 processing site (OPA1ΔS1) with relevant antibodies in mitochondrial lysates from indicated cells, with and without CCCP treatment. **(B)** Extracellular flux analysis of *in vivo* oxygen consumption rates in indicated MEF cells. Cells were cultured in medium containing 10 mM galactose, then transferred into standard Seahorse XF medium and analyzed at 50,000 cells/well under basal, oligomycin A (OLA), FCCP and antimycin A + rotenone stimulated conditions. Error bars, mean ± S.E. of n=4 biological replicates.

Figure S6, related to Figure 6. Apoptotic resistance of *oma1*$^{-/-}$ cells. (A) Quantitative assessment of cell survival by flow cytometry. Indicated cells were cultured in 10 mM glucose or 10 mM galactose-supplemented medium and stained with propidium iodide (PI). Healthy cells were identified as PI-negative. Data represents means ±S.E. of 3 biological replicates. **(B)** Flow cytometry analysis of healthy (Q3: 7-AAD negative, Annexin V-APC negative), early apoptotic (Q1: 7-AAD negative,

Annexin V-APC positive), late apoptotic (Q2: 7-AAD positive, Annexin V-APC positive) and necrotic (Q4: 7-AAD negative, Annexin V-APC positive) cells. Data are presented as mean ±S.E., n=3; *p<0.05, ***p<0.001 by t-test. **(C)** Left: Representative flow cytometry histograms assessing cytochrome *c* release in healthy (Control) and 1 mM staurosporin-treated (+STS) WT and *oma1*$^{-/-}$ fibroblasts. Iso, isotype control used to monitor antibody specificity. 50,000 cells were analyzed in each experiment. Right: Quantitative analysis of mitochondria-bound cytochrome *c* in the cells of interest. Data are presented as mean ±S.E. of 3 independent experiments; *p<0.05, **p<0.01, ***p<0.001 by t-test.

Figure S7, related to Figure 6. Expression of mitoT does not induce mitochondrial fragmentation in *oma1*$^{-/-}$ cells. Representative merged *in vivo* confocal microscopy images of mitochondrial network (visualized with mCherry, red signal) and mitoT-GFP (green signal) in indicated cells. Yellow color indicates signal overlap. Scale bar, 20 μm.

A

Identified ORFs	Unique Peptide Sequences
ATP5B	37
ATP5A1	16
ATAD3	17
PHB1	3
PHB2	4
MIC60	24
SLC25A6	17
PRDX3	3

B

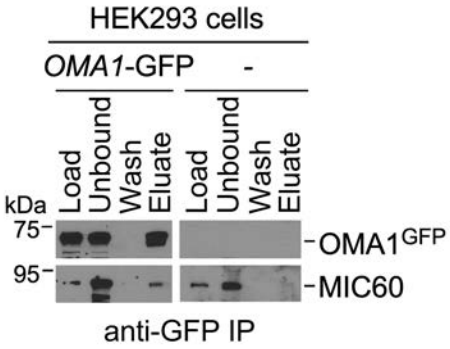

Supplementary figure S1

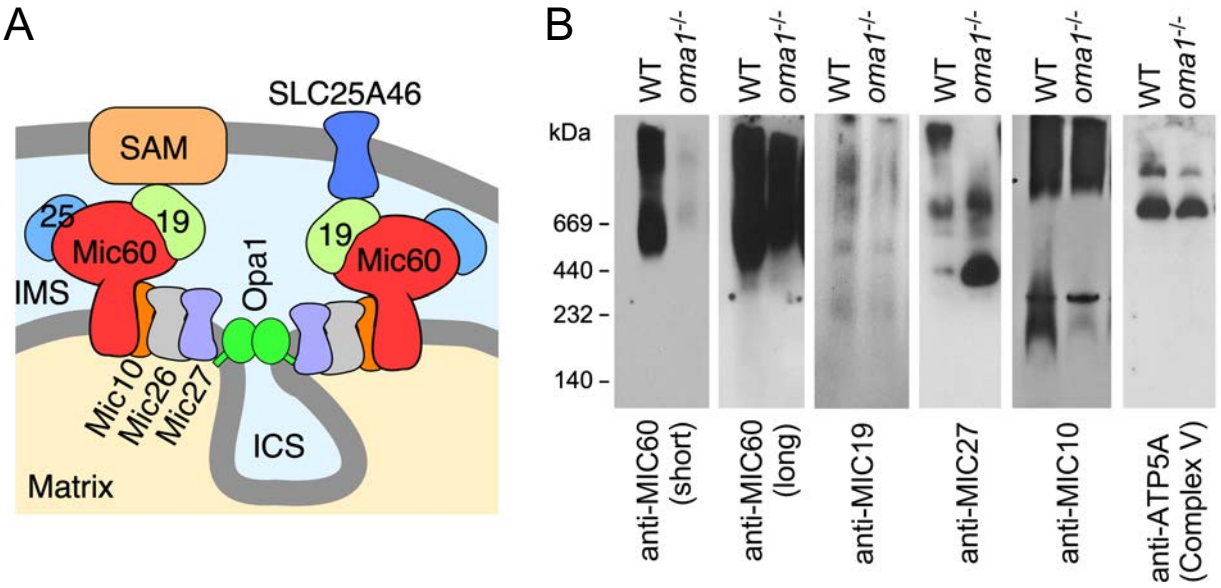

Supplementary figure S2

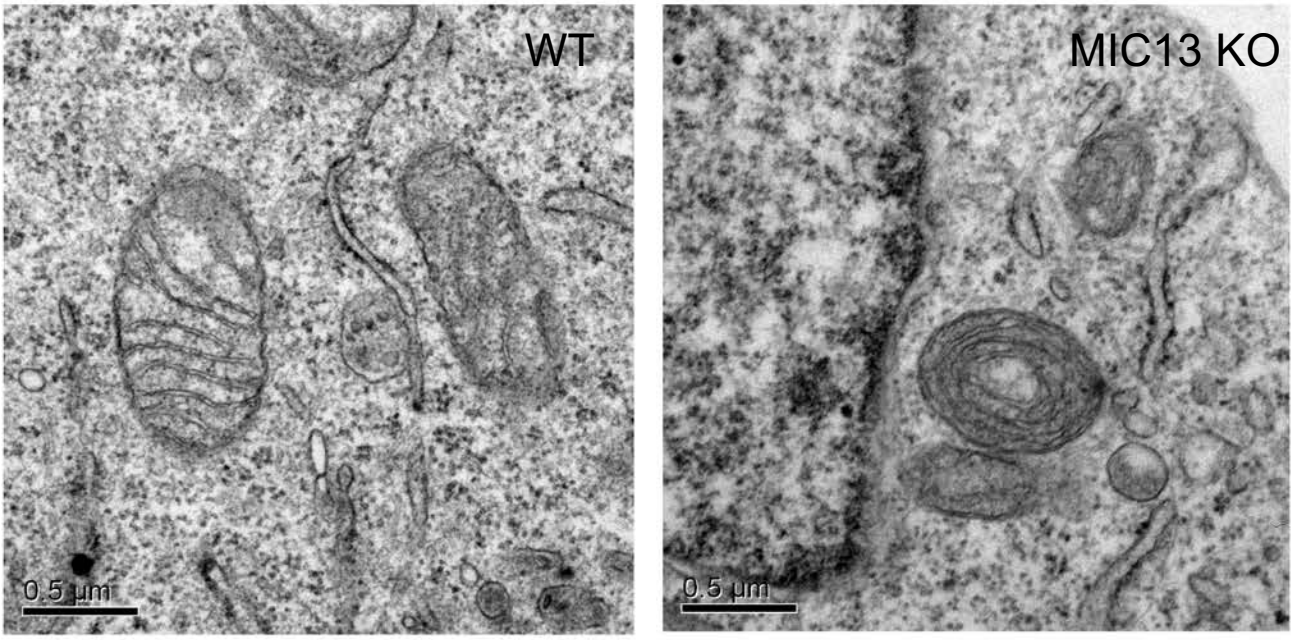

Supplementary figure S3

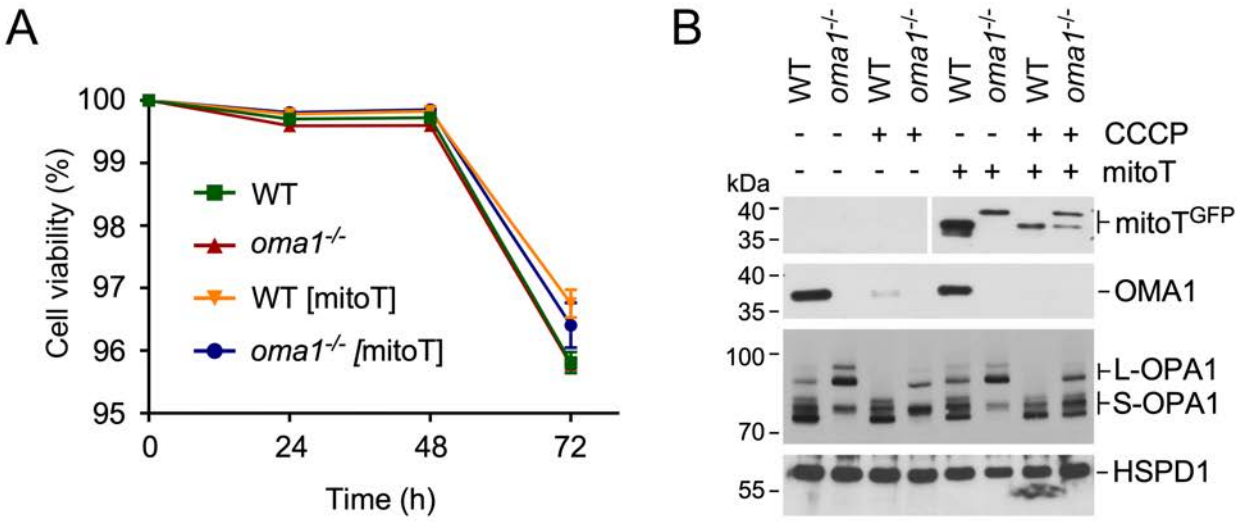

Supplementary figure S4

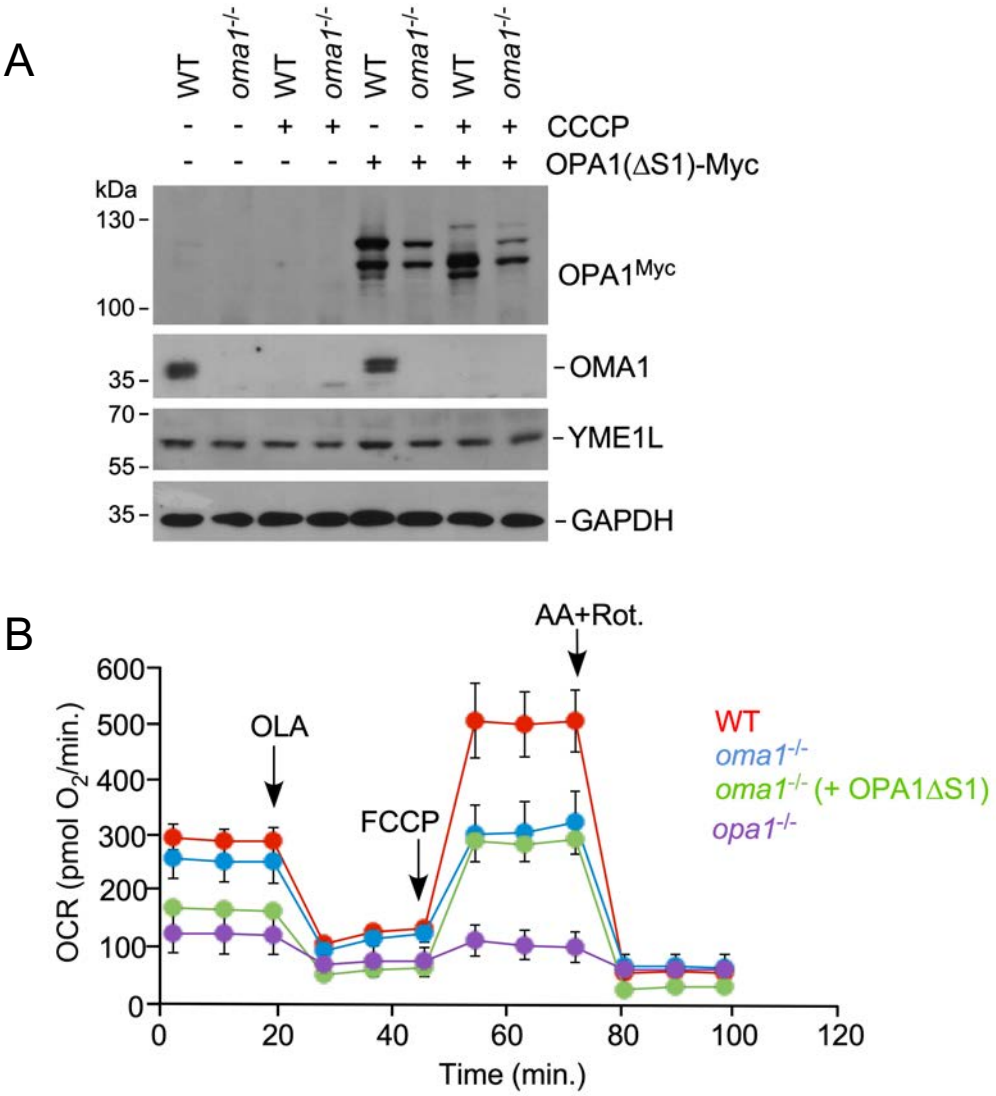

Supplementary figure S5

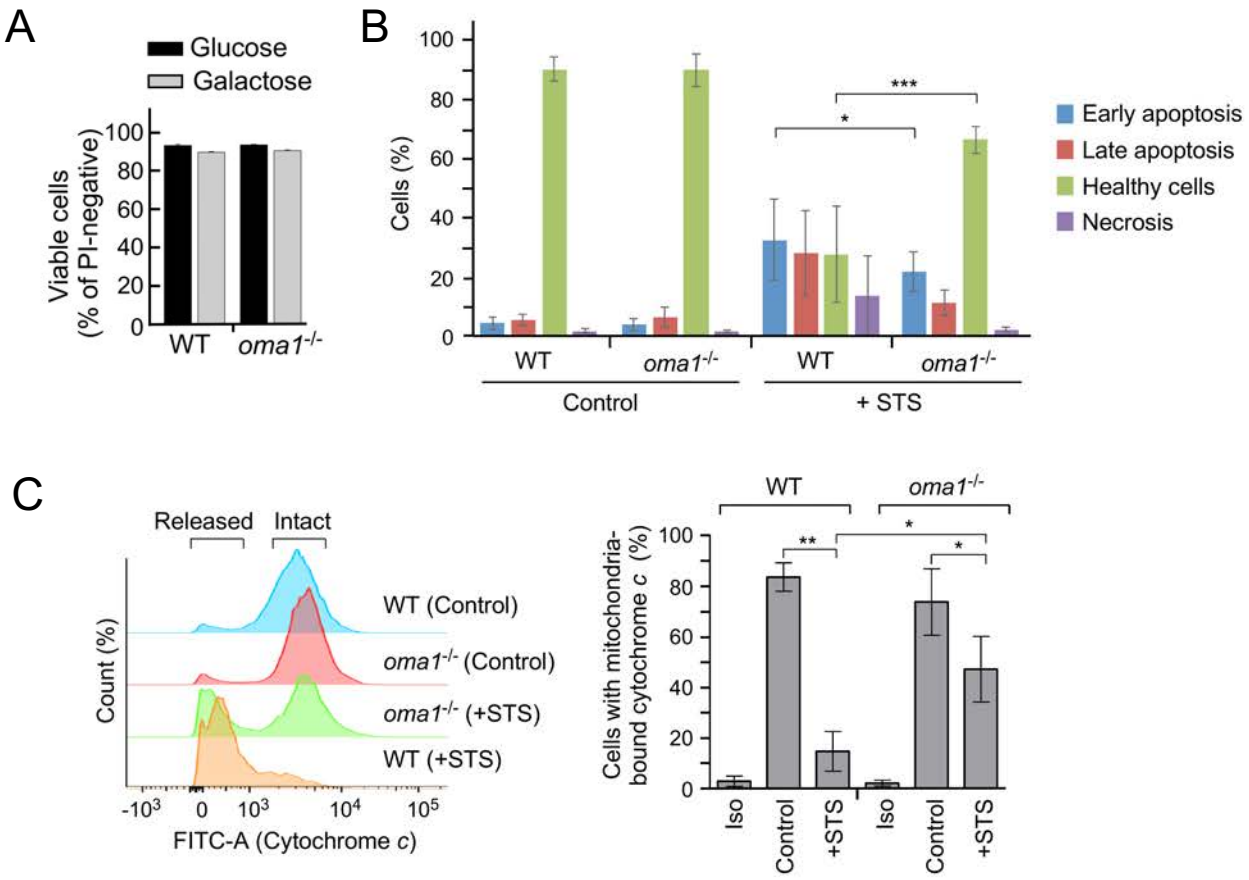

Supplementary figure S6

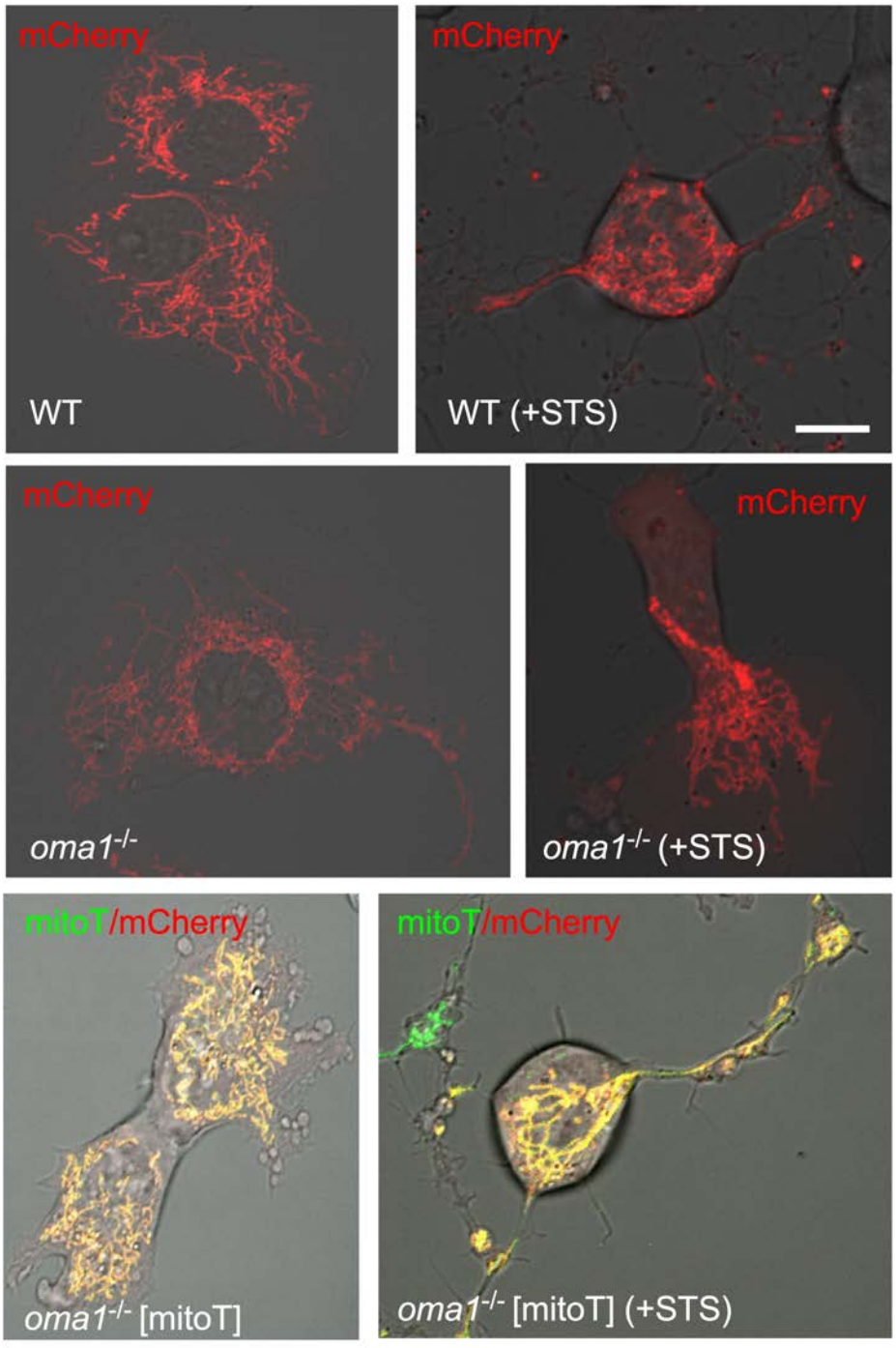

Supplementary figure S7